DYNA
http://dyna.medellin.unal.edu.co/

UNIVERSIDAD NACIONAL DE COLOMBIA

# Theoretical investigation of Hydrogen sulfide adsorption on doped phthalocyanine nanosheets: DFT calculations

Rasha H. Hameed & Mohanned J. Al-Anber

*Molecular Engineering and Computational Modeling Lab, Department of Physics, College of Sciences, University of Basrah, Basrah, Iraq.*
*rasha.hani@uobasrah.edu.iq, mohanned.mohammed@uobasrah.edu.iq*

Received: June 9th, 2025. Received in revised form: December 10th, 2025. Accepted: December 19th, 2025.

**Abstract**
Density functional theory (DFT) computations of phthalocyanine (MePc) monolayers. Utilizing the B3LYP functional alongside a 6-311+G(d,p) basis set, we conducted comprehensive optimization of the molecular structures to evaluate their stability and electrical characteristics. The binding energy between the central metal and the phthalocyanine monolayer was computed, together with the adsorption energy of $H_2S$, to assess the feasibility for gas sensing applications. Our results demonstrate that the adsorption process is primarily spontaneous, with considerable charge transfer occurring during adsorption, as confirmed by Hirshfeld charge calculations. Furthermore, we examined the band-gap energy, global hardness, and electrophilicity index to further the characterization of the sensing capabilities of both pristine and metal-doped phthalocyanine structures. The findings indicate that metal doping improves the sensitivity and stability of phthalocyanine monolayers, making them viable candidates for $H_2S$ detection across diverse applications. This study examines the adsorption characteristics of hydrogen sulfide ($H_2S$) on metal-doped materials.

*Keywords*: hydrogen sulfide ($H_2S$); Phthalocyanine; Density Functional Theory (DFT); gas sensing; metal doping.

# Investigación teórica de la adsorción de sulfuro de hidrógeno en nanohojas de ftalocianina dopadas: cálculos DFT

**Resumen**
Cálculos de la teoría del funcional de la densidad (DFT) de monocapas de ftalocianina (MePc). Utilizando el funcional B3LYP junto con un conjunto de bases 6-311+G(d,p), realizamos una optimización exhaustiva de las estructuras moleculares para evaluar su estabilidad y características eléctricas. Se calculó la energía de enlace entre el metal central y la monocapa de ftalocianina, junto con la energía de adsorción de $H_2S$, para evaluar su viabilidad en aplicaciones de detección de gases. Nuestros resultados demuestran que el proceso de adsorción es principalmente espontáneo, con una considerable transferencia de carga durante la adsorción, como lo confirman los cálculos de carga de Hirshfeld. Además, examinamos la energía de banda prohibida, la dureza global y el índice de electrofilicidad para profundizar en la caracterización de las capacidades de detección de estructuras de ftalocianina, tanto prístinas como dopadas con metal. Los hallazgos indican que el dopaje con metal mejora la sensibilidad y la estabilidad de las monocapas de ftalocianina, lo que las convierte en candidatas viables para la detección de $H_2S$ en diversas aplicaciones. Este estudio examina las características de adsorción del sulfuro de hidrógeno ($H_2S$) en materiales dopados con metal.

*Palabras clave*: sulfuro de hidrógeno ($H_2S$); ftalocianina; Teoría del Funcional de la Densidad (DFT); detección de gases; dopaje de metales.

## 1 Introduction

Hydrogen sulfide ($H_2S$), also known as hydrosulfuric acid, is a colorless and highly toxic gas characterized by a distinct rotten egg odor. It is primarily produced as a byproduct of industrial activities such as natural gas processing, petroleum refining, coal gasification, and biogas fermentation [1,2]. Exposure to $H_2S$ poses serious health

**How to cite:** Hameed, R.H, and Al-Anber, M.J., Theoretical investigation of hydrogen sulfide adsorption on doped phthalocyanine nanosheets: DFT calculations DYNA, (93)240, pp. 46-52, January - March, 2026.

risks, affecting both the nervous system and respiratory tract [3]. At low concentrations, it can cause symptoms like dizziness, nausea, coughing, and chest discomfort [4]. However, higher concentrations may impair olfactory function, leading to a loss of smell and increasing the risk of prolonged exposure, which can result in severe consequences such as organ damage, respiratory failure, and even death [5]. Beyond its health hazards, $H_2S$ also has detrimental environmental and industrial effects. When oxidized to sulfur dioxide ($SO_2$), it contributes to acid rain, damaging crops, infrastructure, and ecosystems. In industrial settings, $H_2S$ accelerates equipment corrosion, degrades catalyst efficiency, reduces product quality, and poses operational hazards [6]. Therefore, accurate and efficient detection of trace $H_2S$ is crucial for ensuring workplace safety, environmental protection, and industrial productivity. Conventional $H_2S$ sensors face limitations such as high energy consumption, low sensitivity, short lifespan, and strict operational conditions [6]. To overcome these challenges, researchers are exploring advanced materials for more reliable and cost-effective gas sensing. Among these, two-dimensional phthalocyanine (Pc) compounds have gained attention due to their unique properties, including high surface area, excellent charge transfer capability, and optical performance [7]. These characteristics make them suitable for applications in photovoltaics [8], optoelectronics [9], electrocatalysis [10], and spintronics [11]. While resistive phthalocyanine-based gas sensors have shown promise in lab settings, their practical use is hindered by poor stability, selectivity, and sensitivity [12]. To enhance their performance, transition metal atoms can be incorporated into the Pc structure, improving their gas-sensing properties [13]. Previous studies using density functional theory (DFT) have demonstrated the effectiveness of metal-doped phthalocyanines—such as zinc phthalocyanine (ZnPc) and chromium phthalocyanine (CrPc)—in detecting gases like CO, NO, and formaldehyde [14,15]. Additionally, Mn-phthalocyanine (MnPc) has been investigated for its interaction with XH3 gases (X = N, P, As) [16]. However, research on metal-doped phthalocyanines for $H_2S$ detection remains limited. This study employs DFT simulations to evaluate the $H_2S$ adsorption behavior on gallium (GaPc), scandium (ScPc), and titanium phthalocyanine (TiPc) monolayers. By analyzing structural configurations, adsorption energies, charge transfer mechanisms, electronic band gaps, and density of states, we assess the potential of these materials for $H_2S$ sensing applications.

## 2 Modeling and computing

Accurate determination of properties such as adsorption energy, dipole moment, and charge transfer necessitate the use of larger basis sets. A reliable approach for modeling molecular configurations involves employing a split-valence double-zeta basis set, exemplified by 6-311+G(d,p), which is a Pople-style basis set [17]. Full geometric optimizations were conducted with the B3LYP functional in conjunction with the 6-311+G(d,p) basis set [18,19]. The B3LYP method integrates Becke's three-parameter hybrid exchange functional (B3) and the Lee-Yang-Parr correlation functional (LYP), making it a widely adopted choice for studying nanostructures, including III-V semiconductor systems [20]. To account for weak long-range interactions, Grimme's D3 dispersion correction with Becke-Johnson damping (DFT-D3(BJ)) was applied [21]. All simulations were carried out using Gaussian 16 [22] within the framework of density functional theory (DFT) [23]. Input preparation and output visualization were facilitated by GaussView 5.0 [24], while density of states (DOS) plots were generated via GaussSum 3.0 [25].

The binding energy ($BE$) of the metal center within the phthalocyanine (Pc) monolayer was calculated as:

$$BE = (E_{MePc} - (E_{Me} + E_{Pc})) \quad (1)$$

where $E_{\mathrm{MePc}}$ and $E_{\mathrm{Pc}}$ represent the total energies of the metal-doped and undoped Pc monolayers, respectively, while $E_{\mathrm{Me}}$ corresponds to the energy of an isolated metal atom [26].

The adsorption energy ($E_{\mathrm{ads}}$) of hydrogen sulfide ($H_2S$) on the Pc and MePc monolayers was computed to assess sensing performance:

$$E_{ads} = E_{gas/MePc} - (E_{gas} + E_{MePc}) \quad (2)$$

where, $E_{gas/MePc}$ is the total energy of the $H_2S$-adsorbed system, whereas $E_{MePc}$ and $E_{gas}$ denote the energies of the isolated MePc monolayer and $H_2S$ molecule, respectively. A negative $E_{\mathrm{ads}}$ typically indicates exothermic adsorption, with greater negativity reflecting stronger stability [27]. Adsorption is classified as chemisorption if $|E_{\mathrm{ads}}|>0.5$eV; otherwise, it is considered physisorption [28]. This investigation evaluated $H_2S$ adsorption on Pc and MePc monolayers at 298.15 K. Additionally, key electronic parameters were analyzed, including the bandgap ($Eg = E_{\mathrm{LUMO}} - E_{\mathrm{HOMO}}$), global hardness ($\eta = Eg/2$), and electrophilicity index ($\omega = (E_{\mathrm{HOMO}} + E_{\mathrm{LUMO}})^2/8\eta$), where $E_{\mathrm{HOMO}}$ and $E_{\mathrm{LUMO}}$ are the energies of the lowest unoccupied and highest occupied molecular orbitals, respectively [20]. The sensitivity of pristine and Me-doped Pc toward $H_2S$ was quantified by the relative change in bandgap:

$$\Delta E_g\% = [(E_{g_2} - E_{g_1})/E_{g_1}] \times 100 \quad (3)$$

Where, $E_{g2}$ and $E_{g1}$ are the bandgap values before and after $H_2S$ adsorption.

To elucidate substrate-gas interactions, Hirshfeld charge analysis was performed to determine charge transfer $Q_{\mathrm{CT}}$:

$$Q_{CT} = Q_{(H2S)_A} - Q_{(H2S)_B} \quad (4)$$

Here, $Q_{(\mathrm{H2S})\mathrm{A}}$ and $Q_{(\mathrm{H2S})\mathrm{B}}$ represent the net charges on $H_2S$ after and before adsorption, respectively. A positive $Q_{\mathrm{CT}}$ implies electron donation from $H_2S$ to the Pc surface, while a negative value suggests the opposite direction of transfer [29].

## 3 Results and discussion

### *3.1 Structure and stability of pristine Pc, MePc, and $H_2S$*

Fig. 1 illustrates the optimized structures of (a) pristine phthalocyanine (Pc), (b) gallium-doped Pc (GaPc), (c)

scandium-doped Pc (ScPc), (d) titanium-doped Pc (TiPc), and (e) an isolated hydrogen sulfide ($H_2S$) molecule. The atomic color scheme is as follows: gray for carbon (C), white for hydrogen (H), blue for nitrogen (N), orange for gallium (Ga), pink for scandium (Sc), green for titanium (Ti), and yellow for sulfur (S). The coplanar configuration of the pristine Pc monolayer indicates a completely delocalized and conjugated π-electron system. Both GaPc and TiPc monolayers exhibit a stable "graphene-like" planar shape, signifying a robust connection between the metal atoms and the Pc nanosheet, consistent with previously reported values [30]. Conversely, the ScPc monolayer shows a pronounced out-of-plane displacement of the Sc atom, resulting in a non-planar structure. The isolated $H_2S$ molecule exhibits an H–S bond length of 1.35 Å and a bond angle of 92.73°, in accordance with previous studies [20]. Among the doped phthalocyanines, TiPc demonstrates the most substantial negative binding energy (*BE*), as illustrated in Fig. 1d, signifying a more robust link between the metal atom and the Pc monolayer relative to ScPc and GaPc. The possibility of metal atom aggregation inside the phthalocyanine monolayer was investigated by calculating the cohesive energy ($E_{coh}$) using the formula:

$$E_{coh} = \frac{E_{MePc} - E_{iso-Me}}{n} \quad (5)$$

$E_{coh}$=($E_{MePc}$-$E_{iso-Me}$)/n, where $E_{iso-Me}$ denotes the energy of an individual metal atom and n indicates the number of metal atoms. The findings demonstrate that TiPc and ScPc possess the greatest cohesive energies, succeeded by GaPc and pure Pc. Fig. 1 presents the EBE values for GaPc, ScPc, and TiPc monolayers as −7.33 eV, −9.67 eV, and −10.97 eV, respectively. All these values are below the cohesive energy of the respective metal bulk, so affirming its stability. Prior research suggests that the central location, particularly the vacancy in the center of Pc or directly above the doped metal atom in MePc, is the favored adsorption site [31]. The stability of an atom on an adsorbent can be defined by its diffusion activation barrier ($E_{act}$). Calculations in machine learning indicate that for individual atoms of diverse metal species on various two-dimensional materials, the energy barriers are proportional to ($BE^2/E_{coh}$). While 2D Pc is excluded from these computations, a preliminary estimation can be obtained from the subsequent equation:

$$E_{act} = 0.63(E_{BE}^2/E_{coh}) - 0.203 \quad (6)$$

In this context, *BE* denotes the binding energy, while Ecoh signifies the cohesive energy of the metal atoms adsorbed on 2D Pc, as depicted in Fig. 1. It is vital that *BE* exceeds $E_{coh}$ to avert the formation of metal clusters on 2D Pc, since this may impair its capacity to interact with other molecules by decreasing the number of accessible adsorption sites. Numerical calculations indicate that Ga, Sc, and Ti exhibit higher *BE* values than their cohesive energies. Moreover, the activation energy exhibits the subsequent trend: Exact: Ti > Sc > Ga. All atomic metals demonstrate binding energies more than 1 eV, signifying substantial interactions with the 2D Pc [32].

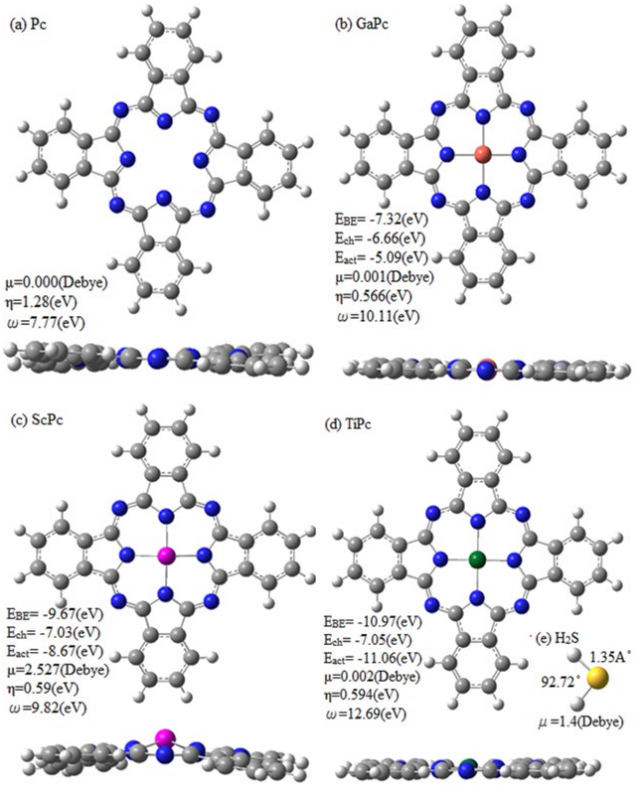


Figure 1. Optimized structures of (a) pristine phthalocyanine (Pc), (b) gallium-doped Pc (GaPc), (c) scandium-doped Pc (ScPc), (d) titanium-doped Pc (TiPc), and (e) hydrogen sulfide ($H_2S$). Color code: gray (C), white (H), blue (N), orange (Ga), pink (Sc), green (Ti), yellow (S).
Source: Authors.

### *3.2 Adsorption properties of $H_2S$ on pristine and metal-doped phthalocyanine*

The optimized adsorption configurations of $H_2S$ on pristine phthalocyanine (Pc) and metal-doped Pc (MePc, where Me = Ga, Sc, Ti) are depicted in Fig. 2. For pure Pc, the calculated adsorption energy ($E_{ads}$) is −7.21 kcal/mol, accompanied by a charge transfer ($Q_{CT}$) of −0.171 e from Pc to $H_2S$ (Fig. 3). This weak interaction indicates primarily physical adsorption, consistent with previous studies [27], and suggests limited $H_2S$ capture capability.

In contrast, doping with Sc and Ti significantly enhances $H_2S$ adsorption. The most stable configurations, $H_2S$+ScPc and $H_2S$+TiPc, exhibit $E_{ads}$ values of −17.22 and −22.70 kcal/mol, respectively, confirming chemisorption [30]. Ga doping, however, does not improve adsorption performance, as reflected in its lower $E_{ads}$ compared to ScPc and TiPc. Structural analysis reveals minimal distortion in $H_2S$ adsorbed on ScPc and TiPc, with adsorption distances of 2.80 Å ($Q_{CT}$ = 0.267 e) and 2.50 Å ($Q_{CT}$ = 0.216 e), respectively. These results demonstrate superior $H_2S$ adsorption on ScPc and TiPc relative to GaPc and pristine Pc. Electronic structure analysis further supports these findings. The HOMO-LUMO gap (*Eg*) of pristine Pc decreases only slightly (2.55 eV → 2.34 eV) upon $H_2S$ adsorption (Fig. 3), indicating low sensitivity for detection. In contrast, Ga, Sc,

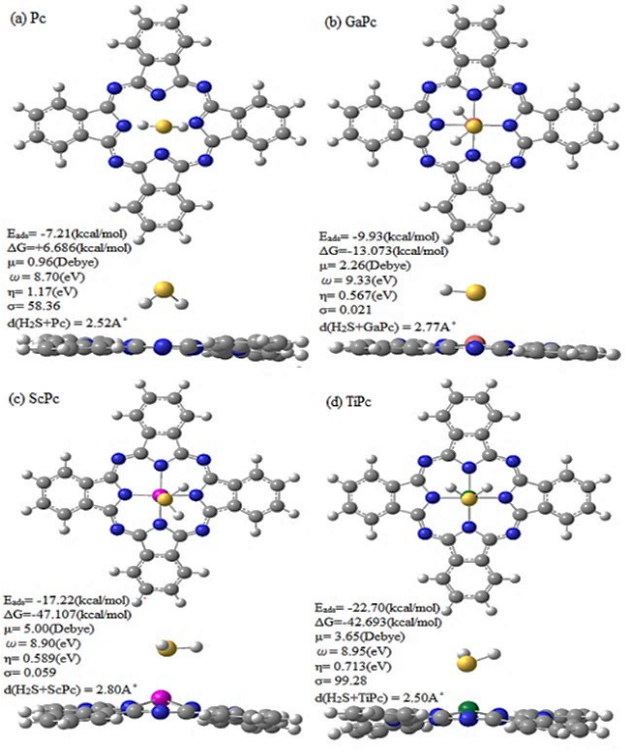


Figure 2. Top and side views of $H_2S$ adsorbed on (a) Pc, (b) GaPc, (c) ScPc, and (d) TiPc. Atom colors: gray (C), white (H), blue (N), orange (Ga), pink (Sc), green (Ti), yellow (S).
Source: Authors.

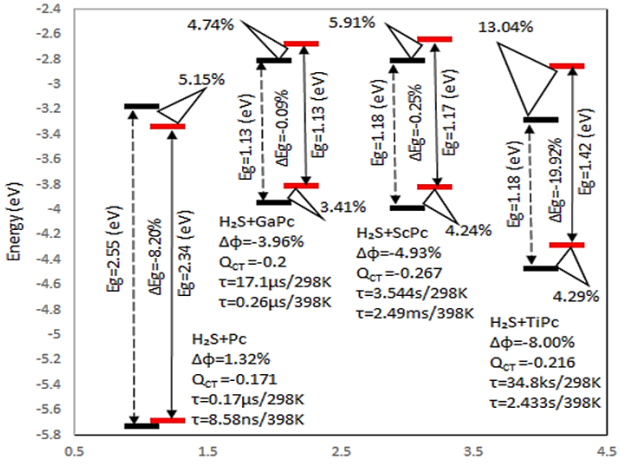


Figure 3. HOMO-LUMO energy levels for $H_2S$ adsorbed on Pc, GaPc, ScPc, and TiPc. Black lines represent systems before adsorption; red lines show post-adsorption states.
Source: Authors.

and Ti doping induces notable shifts in the HOMO level, reducing Eg and enhancing $H_2S$ interaction. Global hardness ($\eta$) measurements reveal minimal changes for GaPc and ScPc after adsorption, whereas TiPc shows significant variations. The electrophilicity index ($\omega$) also undergoes marked shifts, particularly for TiPc+$H_2S$, suggesting TiPc's stronger affinity for $H_2S$. Thermodynamic calculations reveal spontaneous adsorption ($\Delta G < 0$) for all MePc systems, with ScPc (−47.10 kcal/mol) and TiPc (−42.69 kcal/mol) exhibiting the strongest interactions, followed by GaPc (−13.07 kcal/mol). Pristine Pc, however, shows a positive $\Delta G$ (6.68 kcal/mol), indicating non-spontaneous adsorption (Fig. 2).

Density of states (DOS) analysis provides additional insights. For pristine Pc (Fig. 4), $H_2S$ exhibits delocalized states with no significant resonance peaks, indicating weak van der Waals interactions [34] and poor gas-sensing potential. In contrast, ScPc (Fig. 5) and TiPc (Fig. 7) display strong resonance peaks (highlighted by dashed rectangles), confirming robust orbital hybridization. The Sc and Ti atoms act as electron bridges, facilitating charge transfer and strengthening $H_2S$ adsorption. GaPc (Fig. 6) also shows enhanced orbital overlap, though to a lesser extent than ScPc and TiPc. These findings highlight TiPc as a promising candidate for $H_2S$ sensing applications.

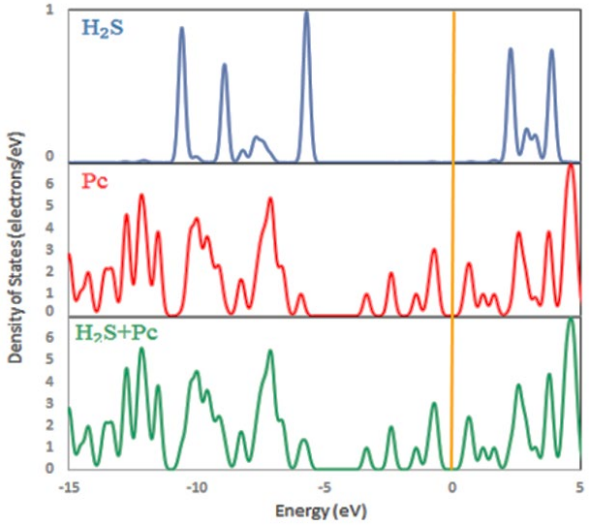


Figure 4. Density of states (DOS) for $H_2S$, Pc, and their combined system. The Fermi level (orange line) is set at zero energy.
Source: Authors.

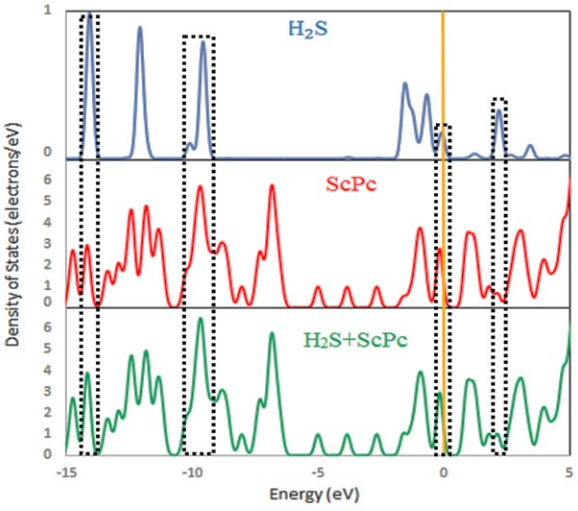


Figure 5. DOS for $H_2S$, ScPc, and their combined system. The Fermi level (orange line) is at zero energy.
Source: Authors.

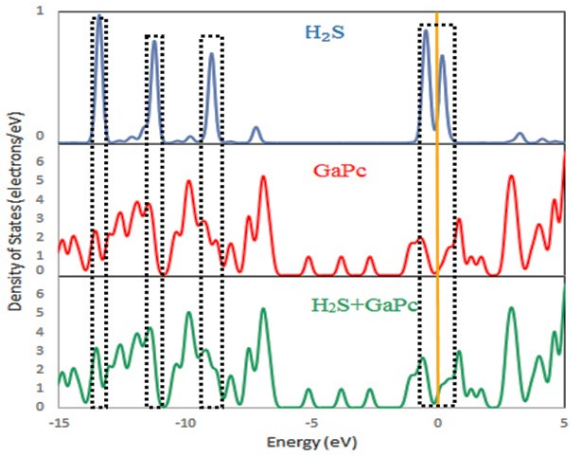


Figure 6. DOS for $H_2S$, GaPc, and their combined system. The Fermi level (orange line) is at zero energy.
Source: Authors.

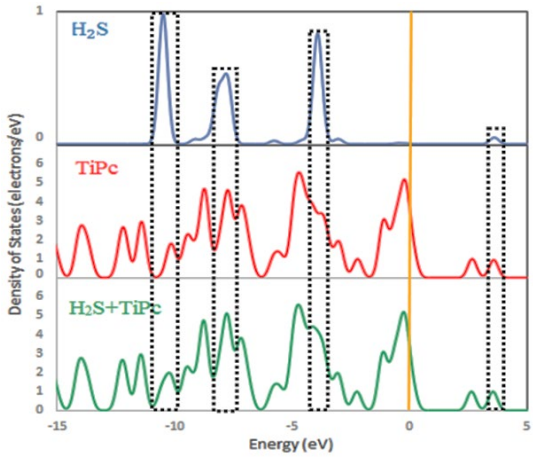


Figure 7. DOS for $H_2S$, TiPc, and their combined system. The Fermi level (orange line) is at zero energy. Source: Authors.

### *3.3 Sensing mechanism analysis*

The preceding sections established the durability and strong adsorption capacity of ScPc and TiPc monolayers, confirming their suitability for $H_2S$ gas sensing. To gain deeper insight into the sensing mechanism, we evaluated the sensitivity and desorption behavior of these monolayers upon $H_2S$ exposure.

The energy gap ($Eg$) serves as an indicator of molecular excitability—a smaller gap corresponds to higher excitation likelihood, reflecting changes in conductivity. As shown in Fig. 3, GaPc and ScPc monolayers exhibit semimetallic behavior, with negligible shifts in their electronic band gaps after $H_2S$ adsorption. This suggests minimal electrical response, indicating low sensitivity. In contrast, the TiPc monolayer undergoes a significant band gap increase from 1.188 eV to 1.425 eV ($\Delta Eg$ = 19.92%) upon $H_2S$ adsorption, transitioning from semimetallic to semiconducting properties. This shift highlights TiPc's superior sensitivity to $H_2S$.

The sensitivity can be quantified by changes in electrical conductivity ($\sigma$), expressed as: $\sigma \propto \exp(-Eg/2k_BT)$, where $Eg$ is the band gap, $k_B$ is the Boltzmann constant ($8.62 \times 10^{-5}$ eV/K), and T the operating temperature. The negligible band gap shift in $H_2S$-ScPc systems results in minimal resistivity changes ($\sigma_{ScPc}$ = 0.059), confirming low sensitivity. Conversely, ScPc and TiPc exhibit notable electronic perturbations upon $H_2S$ exposure, with σ values of 0.059 and 99.28, respectively. The substantial change in TiPc underscores its potential as an $H_2S$ sensor.

We further investigated the influence of $H_2S$ on Fermi levels ($E_F$) and work function ($\phi$), defined as: $\phi = -E_F = (E_{LUMO}+E_{HOMO})/2$. The work function shift ($\Delta\phi$) is critical for ϕ-type sensors, which measure this parameter via Kelvin oscillation. Post-adsorption, Ga-, Sc-, and Ti-decorated 2D Pc exhibit $\Delta\phi$ values of -3.96%, -4.93%, and -8.00%, respectively, while pristine Pc shows a slight increase ($\Delta\phi$ = 1.32%). The most pronounced change occurs in TiPc, followed by ScPc, confirming work function as a key metric for sensor performance.

Desorption kinetics ($\tau$) are equally vital for sensor reusability. Moderate gas-substrate interactions facilitate rapid desorption, ensuring sustained operation. Using transition state theory, we calculated $\tau$ as: $\tau = (f_0)^{-1}\exp(-E_{abs}/k_BT)$, where the attempt frequency $f_0$ is taken as $1\times10^{12}$ $s^{-1}$. For ScPc, $\tau$ values are 3.54 s (298 K) and 2.49 ms (398 K), while TiPc shows slower recovery (34.8 ks at 298 K, 2.43 s at 398 K). ScPc's short recovery time at ambient temperature, combined with adequate sensitivity, makes it a promising candidate for $H_2S$ detection. Comparative studies reveal that hydroxyl-modified ZGNRs exhibit weak $H_2S$ adsorption ($E_{ads}$ = -0.17 eV) [35], while PdAs monolayers show physical adsorption ($E_{ads}$ = -0.49 eV) with a 179 s recovery time [36]. Zinc-doped $SnP_1$ demonstrates faster recovery (64 ms at 298 K) but lower adsorption strength ($E_{ads}$ = -0.639 eV) [37]. In contrast, ScPc offers optimal adsorption and rapid desorption, positioning it as a highly effective $H_2S$ sensor.

### *3.4. Dipole moments of adsorbates and substrates*

The dipole moment ($\mu$) of a molecule plays a crucial role in adsorption behavior by influencing electrostatic forces between the adsorbate and substrate [37]. To analyze these interactions, we computed the dipole moments of $H_2S$ gas, pristine nanosheets, and doped nanosheets. Our results show that $H_2S$ possesses a dipole moment of 1.399 Debye (Fig. 1). Notably, the doped nanosheets exhibit slightly higher $\mu$ values compared to their undoped counterparts (Fig. 2). Among these, the $H_2S$+TiPc system shows the most pronounced increase in dipole moment. This enhancement correlates with stronger adsorption energies, suggesting that doping improves $H_2S$ adsorption via intensified electrostatic interactions.

## 4 Conclusion

This study employed density functional theory (DFT) calculations to systematically investigate the structural, electronic, and adsorption properties of pristine and metal-doped phthalocyanine (Pc) monolayers for hydrogen sulfide ($H_2S$) sensing applications.

The results demonstrate that doping with transition metals significantly enhances the stability and gas adsorption performance of Pc nanosheets compared to the pristine structure. Among the studied dopants (Ga, Sc, Ti), Sc and Ti

incorporation proved most effective, yielding strong binding energies and spontaneous, exothermic $H_2S$ adsorption indicative of chemisorption. In contrast, Ga doping and the pristine Pc monolayer showed only weak, physisorptive interactions with $H_2S$.

Electronic structure analysis revealed that ScPc and TiPc undergo substantial charge transfer and orbital hybridization upon $H_2S$ exposure. A critical finding is the pronounced change in the electronic band gap of TiPc, which shifts from semimetallic to semiconducting character after adsorption. This significant alteration in electronic properties, coupled with a notable change in work function, suggests a strong electrical response to the target gas, which is essential for resistive and work-function-based sensing mechanisms. Furthermore, analysis of recovery times indicates that ScPc offers an optimal balance between adequate adsorption strength and rapid desorption at ambient temperature, promoting sensor reusability.

In summary, while both ScPc and TiPc monolayers exhibit superior $H_2S$ adsorption and electronic sensitivity, TiPc emerges as the most promising candidate due to its strongest adsorption energy and the most significant modulation of its electronic properties. These characteristics recommend TiPc-doped phthalocyanine nanosheets as highly suitable materials for the development of efficient, sensitive, and reusable $H_2S$ gas sensors.

## References


[1] Ganji, M.D., and Danesh, N., Adsorption of $H_2S$ molecules by cucurbit [7] uril: an ab initio vdW-DF study. RSC Advances, 3(44), pp. 22031-22038, 2013. DOI: https://doi.org/10.1039/c3ra41946k.

[2] Drummer, O.H., Disposition of toxic drugs and chemicals in man. Australian Journal of Forensic Sciences, 41(2), p. 163, 2009. DOI: https://doi.org/10.1080/00450610903019561.

[3] Shefa, U., Kim, M.S., Jeong, N.Y., and Jung, J., Antioxidant and cell-signaling functions of hydrogen sulfide in the central nervous system. Oxidative medicine and cellular longevity, Art. 1873962, 2018. DOI: https://doi.org/10.1155/2018/1873962.

[4] Lashgari, M., and Ghanimati, M., Photocatalytic degradation of $H_2S$ aqueous media using sulfide nanostructured solid-solution solar-energy-materials to produce hydrogen fuel. Journal of Hazardous Materials, 345, pp. 10-17, 2018. DOI: https://doi.org/10.1016/j.jhazmat.2017.10.062.

[5] Ayesh, A.I., et al., Selective gas sensors using graphene and CuO nanorods. Sensors and Actuators A: Physical, 283, pp. 107-112, 2018. DOI: https://doi.org/10.1016/j.sna.2018.09.068.

[6] [6] Sharma, S., and Verma, A.S., A theoretical study of $H_2S$ adsorption on graphene doped with B, Al and Ga. Physica B: Condensed Matter, 427, pp. 12-16, 2013. DOI: https://doi.org/10.1016/j.physb.2013.05.019.

[7] Zhang, R., Lu, L., Chang, Y., and Liu, M., Gas sensing based on metal-organic frameworks: concepts, functions, and developments. Journal of Hazardous Materials, 429, Art. 128321, 2022. DOI: https://doi.org/10.1016/j.jhazmat.2022.128321.

[8] Jin, L., and Chen, D., Enhancement in photovoltaic performance of phthalocyanine-sensitized solar cells by attapulgite nanoparticles. Electrochimica, 72, pp. 40-45, 2012. DOI: https://doi.org/10.1016/j.electacta.2012.03.167.

[9] Darwish, A.A.A., et al., Linear and nonlinear optical characteristics of manganese phthalocyanine chloride/polyacetate sheet: Towards flexible optoelectronic devices. Optical Materials, 114, Art. 110988, 2021. DOI: https://doi.org/10.1016/j.optmat.2021.110988.

[10] Huang, S., Chen, K., and Li, T.T., Porphyrin and phthalocyanine based covalent organic frameworks for electrocatalysis. Coordination Chemistry Reviews, 464, Art. 214563, 2022. DOI: https://doi.org/10.1016/j.ccr.2022.214563.

[11] Zemła, M.R., Czelej, K., and Majewski, J.A., Graphene−iron (II) phthalocyanine hybrid systems for scalable molecular spintronics. The Journal of Physical Chemistry C, 124(50), pp. 27645-27655, 2020. DOI: https://doi.org/10.1021/acs.jpcc.0c06949.

[12] Alosabi, A.Q., Al-Muntaser, A.A., El-Nahass, M.M., and Oraby, A.H., Structural, optical and DFT studies of disodium phthalocyanine thin films for optoelectronic devices applications. Optics & Laser Technology, 155, 108372, 2022. DOI: https://doi.org/10.1016/j.optlastec.2022.108372.

[13] Zhou, Y., Gao, G., Chu, W., and Wang, L.W., Computational screening of transition metal-doped phthalocyanine monolayers for oxygen evolution and reduction. Nanoscale Advances, 2(2), pp. 710-716, 2020. DOI: https://doi.org/10.1039/c9na00648f.

[14] Chaabene, M., et al., Insights into theoretical detection of CO2, NO, CO, O2, and O3 gases molecules using Zinc phthalocyanine with peripheral mono and tetra quinoleinoxy substituents: Molecular geometries, Electronic properties, and Vibrational analysis. Chemical Physics, 547, Art. 111198, 2021. DOI: https://doi.org/10.1016/j.chemphys.2021.111198.

[15] Long, D.B., et al., Two-dimensional bimetal-embedded expanded phthalocyanine monolayers: a class of multifunctional materials with fascinating properties. Advanced Functional Materials, 34(22), art. 2313171, 2024. DOI: https://doi.org/10.1002/adfm.202313171.

[16] Badran, H.M., Eid, K.M., Al-Nadary, H.O., and Ammar, H.Y., DFT-D3 and TD-DFT Studies of the Adsorption and Sensing Behavior of Mn-Phthalocyanine toward NH3, PH3, and AsH3 Molecules. Molecules, 29(10), art. 2168, 2024. DOI: https://doi.org/10.3390/molecules29102168.

[17] Resan, S., Hameed, R., Bahrani, F., and Al-Anber, M., Nonlinear optical response of anthracene as a D-π-A conjugated system: Quantum computation study. In: AIP Conference Proceedings, AIP Publishing, 2023. DOI: https://doi.org/10.1063/5.0163185.

[18] Becke, A.D., Density-functional thermochemistry. I. The effect of the exchange-only gradient correction. The Journal of Chemical Physics, 96(3), pp. 2155-2160, 1992. DOI: https://doi.org/10.1063/1.462066.

[19] Frisch, M.J., Pople, J.A., and Binkley, J.S., Self-consistent molecular orbital methods 25. Supplementary functions for Gaussian basis sets. The Journal of Chemical Physics, 80(7), pp. 3265-3269, 1984. DOI: https://doi.org/10.1063/1.447079.

[20] Jia, X., Zhang, H., Zhang, Z., and An, L., First-principles investigation of vacancy-defected graphene and Mn-doped graphene towards adsorption of $H_2S$. Superlattices and Microstructures, 134, art. 106235, 2019. DOI: https://doi.org/10.1016/j.spmi.2019.106235.

[21] Sato, T., and Nakai, H., Density functional method including weak interactions: dispersion coefficients based on the local response approximation. The Journal of Chemical Physics, 131(22), art. 224104, 2009. DOI: https://doi.org/10.1063/1.3270198.

[22] Frisch, M.J., et al., Gaussian 16, Revision C.01. Gaussian, Inc., Wallingford CT, 2016.

[23] Al-Anber, M., Al-Mowali, A., and Ali, A., Theoretical semiempirical study of the nitrone (anticancer drug) interaction with fullerene C60 (as delivery). Acta Physica Polonica A, 126(3), pp. 845-848, 2014. DOI: https://doi.org/10.12693/APhysPolA.126.845.

[24] Dennington, R., Keith, T., and Millam, J., GaussView, Version 5. Semichem Inc., Shawnee Mission, KS, 2009.

[25] Vinod, H.D., Review of GAUSS for Windows, including its numerical accuracy. Journal of Applied Econometrics, 15(2), pp. 211-220, 2000. DOI: https://doi.org/10.1002/(SICI)1099-1255(200003/04)15:2<211::AID-JAE573>3.0.CO;2-4.

[26] Resan, S., Hameed, R., Al-Hilo, A., and Al-Anber, M., The impact of torsional angles to tune the nonlinear optical response of chalcone molecule: Quantum computational study. Revista Cubana de Física, 37(2), pp. 95-100, 2020.

[27] Wang, C., Wang, Y., Guo, Q., Dai, E., and Nie, Z., Metal-decorated phthalocyanine monolayer as a potential gas sensing material for phosgene: a first-principles study. ACS Omega, 7(25), pp. 21994-22002, 2022. DOI: https://doi.org/10.1021/acsomega.2c02548.

[28] Yong, Y., Cui, H., Zhou, Q., Su, X., Kuang, Y., and Li, X., C2N monolayer as NH3 and NO sensors: a DFT study. Applied Surface Science, 487, pp. 488-495, 2019. DOI: https://doi.org/10.1016/j.apsusc.2019.05.040.

[29] Ammar, H.Y., Badran, H.M. and Eid, K.M., TM-doped B12N12 nano-cage (TM = Mn, Fe) as a sensor for CO, NO, and NH3 gases: A DFT

and TD-DFT study. Materials Today Communications, 25, Art. 101681, 2020. DOI: https://doi.org/10.1016/j.mtcomm.2020.101681.

[30] Vozzi, C., et al., Generalized molecular orbital tomography. Nature Physics, 7(10), pp. 822-826, 2011. DOI: https://doi.org/10.1038/nphys2029.

[31] Zhao, W., Zou, D., Sun, Z., Yu, Y., and Yang, C., Controlling spin off state by gas molecules adsorption on metal-phthalocyanine molecular junctions and its possibility of gas sensor. Physics Letters A, 382(37), pp. 2666-2672, 2018. DOI: https://doi.org/10.1016/j.physleta.2018.06.028.

[32] Cid, B.J., et al., Metal-decorated siligene as work function type sensor for NH3 detection: A DFT approach. Applied Surface Science, 610, art. 155541, 2023. DOI: https://doi.org/10.1016/j.apsusc.2022.155541.

[33] Opi, M.H., Ahmed, T., Swarna, M.R., Piya, A.A., and Shamim, S.U.D., Assessment of the drug delivery potential of graphene, boron nitride and their in-plane doped structures for hydroxyurea anti-cancer drug via DFT study. Nanoscale Advances, 20, art. 428, 2024. DOI: https://doi.org/10.1039/D4NA00428K

[34] Berland, K., Cooper, V.R., Lee, K., Schröder, E., Thonhauser, T., Hyldgaard, P., and Lundqvist, B.I., van der Waals forces in density functional theory: The vdW-DF method. *Reports on Progress in Physics*, 78(6), art. 066501, 2015. DOI: https://doi.org/10.1088/0034-4885/78/6/066501.

[35] Salih, E., and Ayesh, A.I., DFT investigation of $H_2S$ adsorption on graphene nanosheets and nanoribbons: Comparative study. Superlattices and Microstructures, 146, art. 106650, 2020. DOI: https://doi.org/10.1016/j.spmi.2020.106650.

[36] Raval, D., Gupta, S.K., and Gajjar, P.N., Detection of $H_2S$, HF and H2 pollutant gases on the surface of penta-PdAs2 monolayer using DFT approach. Scientific Reports, 13(1), art. 586, 2023. DOI: https://doi.org/10.1038/s41598-023-27893-w.

[37] Cui, H., et al., DFT Study of Zn-Modified SnP3: A $H_2S$ Gas Sensor with Superior Sensitivity, Selectivity, and Fast Recovery Time. Nanomaterials, 13(20), art. 2781, 2023. DOI: https://doi.org/10.3390/nano13202781.

**R.H. Hameed** has a PhD in theoretical nanotechnology (2025) from the University of Basra, Iraq. She received the MSc in Physics in 2009. She is currently working on biosensor design, focusing on manufacturing by transition metal according to computational methods.
ORCID: 0000-0002-4844-2313

**M.J. Al-anber** received the BSc in Physics in 1995, the MSc in Physics in 2000, and the PhD in Physics in 2005, all from the University of Basrah, Iraq. From 1997 to 2008, he worked in technical and academic roles, including defense systems research, before joining the University of Basrah as a faculty member. He completed postdoctoral research (2014–2017) on the dielectric properties of titanium dioxide nanorods at the University of Hull, UK. Currently, he is a Professor of Molecular Quantum Dynamics and Statistical Thermodynamics at the University of Basrah. His research interests include: molecular quantum dynamics and electronic structure of macromolecules; dielectric properties of nanomaterials, particularly titanium dioxide nanorods; and statistical thermodynamics of complex systems.
ORCID: 0000-0001-9093-6811